Characterization of CuInS$_2$ Thin Films Grown by
Transducer-based Ultrasonic Spray Pyrolysis for PV Solar Cells Applications

Eric Nguwuo Petuenju[†] and Oumarou Savadogo[*]

Laboratory of New Materials for Energy and Electrochemistry systems (LaNoMat),
Metallurgical Program, Ecole Polytechnique of Montreal, 2900, boul. Édouard-Montpetit, Campus de l'Université de Montréal
2500, chemin de Polytechnique Montréal (Québec), H3T 1J4

Abstract: *For the first time, the elaboration of CuInS$_2$ thin films was achieved using the transducer-based ultrasonic spray pyrolysis method with methanol as solvent. Precursor solutions were prepared with copper dichloride dihydrate [CuCl$_2$.2H$_2$O], indium (III) chloride tetrahydrate [InCl$_3$.4H$_2$O] and thiourea [SC(NH$_2$)$_2$] at different ratios. In$_2$S$_3$ clusters (μdots) were obtained from an aqueous solution with precursors ratio Cu:In:S = 1.3:1:3.9, 1.4:1:3.9, 1.5:1:3.9. CuInS$_2$ thin films were obtained from a solution of methanol with precursors ratio Cu:In:S = 1:1:4. The In concentration was 3 x 10^{-3} mol/l. The crystalline structure and their morphology ware characterised by SEM and their chemical composition by EDAX, The bandgap of CuInS$_2$, equals to 1.40 eV, was determined by spectrophotometry.*

1. INTRODUCTION

Chalcogenide photovoltaic materials are highly relevant candidates for the future of thin film solar cells technology due to their specific advantages: 1) Their synthesis process can be done at low temperature and; 2) they exhibit high tolerance to defects and impurities.

Among this type of materials CuInS$_2$ (CIS), which is a ternary compound I-III-VI$_2$ semiconductor with a chalcopyrite structure, presents a great potential as an absorber layer for photovoltaic solar cell technology applications. Other advantages [1] of this materials are: i) it's high chemical and thermal stability, ii) the value of its optical gap between 1.45 – 1.53 eV, which is close to the optimal theoretical value for the conversion of solar energy (1.5 eV), iii) it exhibits a direct band structure with a high absorption coefficient $\alpha = 5 \times 10^2 - 5 \times 10^5$ cm^{-1} with allowed direct electronic transitions.

The heterojunctions of this material with n-type TiO$_2$ gave very good results in the 3D solar cells technology [2] with a surface active efficiency in the order of 12.5% [3]. However there is a big challenge in the realisation of a nanoscale interpenetrating network of n-type and p-type semiconductors by the "deposition of the p-type material inside the n-type nanoporous matrix" [4]. The realisation of that network is an important aspect in the research on ETA (extremely thin absorber) for application in the technology of 3D solar cells.

Deposition of p-type CuInS$_2$ inside n-type TiO$_2$ pores has been realised using Atomic Layer Chemical Vapor Deposition (ALCVD) [5] and Ion Layer Gas Reaction (ILGAR) [6] without clogging the pores. However, there is a technique that doesn't need vacuum like ALCVD or sulfurization like ILGAR. This alternative technique is the transducer-based ultrasonic spray pyrolysis method [7, 8]. This technique has similar principle but is more environmentally friendly, can be used in open air, is low-cost and easy to use.

Among the low-cost methods used to grow chalcogenide thin films, chemical "spray pyrolysis technique is one of the best-investigated non-vacuum deposition processes" [9]. It is very effective for the preparation of a wide array of materials and has the advantage of being highly scalable and continuous [10]. There are three types of spray pyrolysis (SP): air blasting, ultrasonic and electric field assisted SP [11]. They are based on the use of different types of nebulizers: pneumatic, ultrasonic and electrostatic respectively. Ultrasonic nebulizer has been favored because of its

To whom correspondence should be addressed:
Email: *oumarou.savadogo@polymtl.ca, †eric.nguwuo-petuenju@polymtl.ca

outstanding energy efficiency in aerosol generation, affordability and the inherent low velocity of the initially formed aerosol [10]. There are two types of ultrasonic spray pyrolysis: impact nozzle and actuator (transducer). The deposition of thin films, like $CuInS_2$, by impact nozzle-based ultrasonic spray pyrolysis (INUSP) has already been reported [12] as well as the growth of thin films, like In_2S_3, by actuator-based ultrasonic spray pyrolysis (AUSP) [8, 13]. These techniques are differentiated by the droplets sizes, the droplets distribution and droplets delivery. The droplets sizes, generated by INUSP technique, are in the range of 10 to 1000 μm with a medium distribution and a medium to high delivery, while those generated by the AUSP technique are in the range of 1 to 10 μm with a narrow distribution and a medium delivery [10]. It has been shown that the droplet size [14] as well as the solvent used [15, 16] have a big impact on the quality of the film grown by spray pyrolysis.

The deposition of $CuInS_2$ thin films by transducer-based ultrasonic spray pyrolysis (TUSP), to our knowledge, has never been reported elsewhere. The present work aimed to use the TUSP to grown $CuInS_2$ thin films on transparent and conductive ITO (Indium Tin Oxide) coated glass. The obtained thin films have been characterized. The influence of the nature of the solvent used on the nature of the grown films has been investigated.

2. EXPERIMENTAL DETAILS

The experiments were achieved on a custom-made transducer-based ultrasonic spray pyrolysis (TUSP) system (figure 1). The experimental setup consists of a container in which the solution containing the precursors is introduced. This container is placed above an ultrasonic transducer from piezoelectric system (TDK nebulizer unit NB-80E-01) which transforms the solution into a mist that will be transported through a Teflon pipe by a carrier gas, the nitrogen, to the substrate in a floating movement. The substrate is placed on a heater within the so-called spray chamber. The precursors solution consists of copper dichloride dihydrate [$CuCl_2.2H_2O$], indium (III) chloride tetrahydrate [$InCl_3.4H_2O$] and thiourea [$SC(NH_2)_2$] dissolved and mixed in different solvents such as water and methanol. [$CuCl_2.2H_2O$], [$InCl_3.4H_2O$] and [$SC(NH_2)_2$] were obtained from Sigma-Aldrich. Methanol was obtained from "Les Alcools de commerces, Boucherville, Canada". For the aqueous solution the precursors ratio concentrations was Cu:In:S = 1.2:1:3.6, 1.3:1:3.9, 1.4:1:3.9, 1.5:1:3.9. For the methanol solution, the precursor's ratio was Cu:In:S = 1:1:4. The In concentration was 3×10^{-3} mol/l, the carrier gas flow was 7 ml/sec. The distance, between the nozzle and the substrate, takes different values such as 30, 50, 70 and 90 mm. The heater temperature was 340 °C so that the substrate has a temperature of 300 °C ± 10 °C.

The precursor's solution is sprayed for three minutes (sample CIS1) and seven minutes (sample CIS2) at room temperature to wet the surface prior to the deposition process. That allows the growth process to take place because it facilitates the adherence of the elements at the surface so that the growth can start. Then the substrate heating starts and it takes the heater about seven to eight minutes to reach 340° C. At this temperature, the spraying was pursued for 20 more minutes and we succeeded in growing thin films. The total deposition time was around 30 minutes.

Prior the deposition, the substrate were cleaned by immersion in an ultrasonic acetone bath for 15 minutes, then in an ultrasonic deionised water bath for 15 minutes and, after, dried with air.
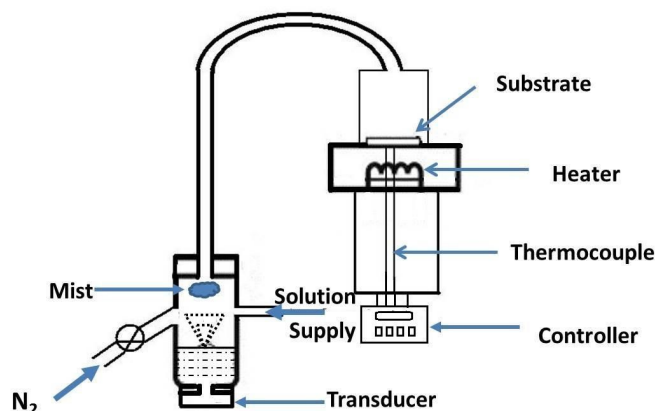
Figure 1. Scheme of the experimental setup for TUSP

The structural and chemical characterizations were done using a Philips X'PERT X-ray diffractometer for structural analysis; the chemical and morphological analysis was done on a scanning electron microscope equipped with an Energy-dispersive X-ray spectrometer, the JEOL JSM840. The optical Analysis was pursued in the Varian Cay 6000i spectrophotometer in the wavelength in the range from 200 to 1000 nm. The thin films resistivity was determined using the four points probe technique with a system setup using Bridgetech probes, a Keithley 220 current source, an Agilent 34401A voltmeter, and a Temptronic TP3000 temperature controller.

3. RESULTS AND DISCUSSION

Based on various deposition conditions, the experimental results have shown that when the aqueous precursor solution contains a Cu/In ratio equal or lower than 1.2, there was no film growth. Concerning the relation between copper and sulfur, for an S/Cu ratio upper than 3, there was also no film growth. The growth of films starts with a precursor solution containing a ratio Cu:In:S = 1.2:1:3.6. It is illustrated by an immediate response during the simultaneous mixing of three precursor solutions with a precipitation of a white solution. This indicates that the concentration ratios are appropriate for obtaining a thin layer.

In the case of the alcoholic precursor solution, for Cu/In = 1 and S/Cu < 4, there is an immediate and irreversible reaction between Cu and S that leads to a solution saturated with Cu_xS_y precipitate. Due to the resulting density, supply of container in solution becomes as difficult as the precursor solution transformation into a mist becomes impossible. For the S/Cu ≥ 4, there is also a formation of Cu_xS_y precipitate. But in this case, the reaction is reversible by stirring the solution for less than 1 minute. Afterwards, the solution remains stable and can be stored for several days. The precursors ratio, in this following work, was Cu:In:S = 1:1:4.

The gas flow was chosen equal to 7 ml/sec because it allows an aerosol with a buoyant aspect. There is no film growth when the gas flow is kept equal to 7 ml/sec, for a distance nozzle-substrate d ≤ 50 mm and d ≥ 90 mm. The reason is: for d ≤ 50 mm, the spray jet is strong enough to expel precursor from the surface. In the case of d ≥ 90 mm, thermophoretic forces overcome the gravity of the drops so that the reaction between precursors occurs before the

a)

b)

c)
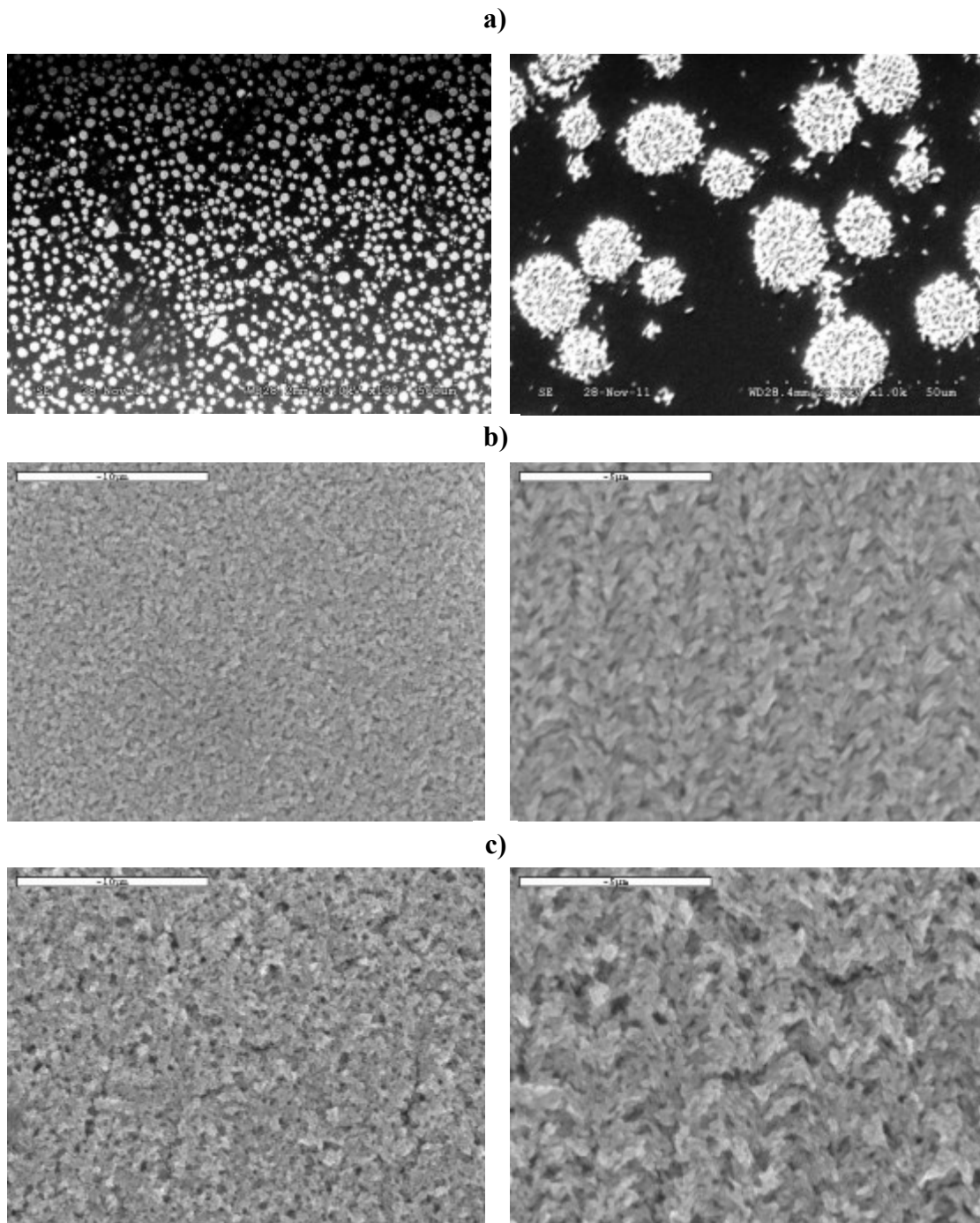
Figure 2. SEM pictures of obtained samples: a) from aqueous precursor solution, b) with methanol as solvent with 3 minutes of wetting the substrate surface (CIS1), c) with methanol as solvent with 7 minutes of wetting the substrate surface (CIS2).

substrate surface and the resulting powder is vented from the surface. The film growth occurs for 60 mm ≤ d ≤ 80 mm. In this work, the nozzle-substrate distance vas chosen d = 70 mm.

Fig.2 shows the SEM images of the deposited films with water solvent (Fig.2a) and methanol (Fig.2b and 2.c), respectively. Their morphology depends on the solvent used for the deposition of the obtained thin films. As seen in the figure 2.a, the deposit from the

aqueous precursor solution are clusters (μ-dot), with an average diameter of few micrometers (3 to 20 μm) while the deposit from the alcoholic (methanol) precursor solution is a non-porous thin film (figure 2.b (with 3 minutes of wetting the substrate surface - CIS1), figure 2.c (with 7 minutes of wetting the substrate surface - CIS2)). The sample CIS1 exhibits a good homogeneous morphology while sample CIS2 presents some cracks or pinholes on its sur-

face. This is a clear indication that the uniformity of the film is related to the surface's relative humidity conditions; and consequently it is related to the surface tension which impacts the droplets' diameter as shown below.

In the spray pyrolysis process, the desire is to have the most possible droplets strike the substrate and spread [11]. The droplets size and the spreading behavior of the droplets on the surface are determined by the surface tension of the solvent. Accordingly, using Lang's correlation between droplet diameter, the surface tension and solvent density at a constant fraction of the capillary wavelength in the exiting frequency, we can estimate the value of each parameter on this diameter with the following equation [11, 17, 18]:

$$D = 0.34 \left(\frac{8\pi\sigma}{\rho f^2} \right)^{1/3} \qquad (1)$$

where D (m) is the droplet size, 0.34 is the empirically found constant fraction, σ (N/m) - the surface tension of the solvent ρ (kg/m^3) - the density of the solvent and f (Hz) is the excitation frequency.

Table 1 shows that the surface tension of water (71.97 x 10^{-3} N/m) is more than 3 times superior to the surface tension of methanol (22.5 x 10^{-3} N/m). Also the density of water (1ton/m^3) is superior to the density of methanol (791 kg/m^3).

The calculated droplet sizes, using eq. (1) at a temperature of 25 °C, are listed in table 1. For the same experimental conditions, the droplet diameter of deposits done with water solvent is higher than those obtained with methanol.

If we consider that the substrate has a temperature of 300 °C during the experiments, methanol may evaporate faster than water. Considering the surface tension, it seems that the water droplets spend more time at the substrate surface than those of methanol which might spread and evaporate rapidly. Due to the volatility of methanol, before the droplets reach the substrate, the concentrations of precursors in the solvent increase as the quantity of methanol decreases. Then the final reaction between the precursors occurs at the surface, facilitating agglomeration and the growth of a thin film. With water, the reaction occurs in the solvent at the substrate surface and lead to a deposition of isolated clusters (figure 2.a), after the evaporation of water. Then, the difference in the obtained materials is linked to the nature of the solvents and the incidence of the transducer. Methanol acts like an inhibitor and reduces the kinetic of the reaction between copper and sulfur. With the aqueous solvent, the vibrations of the piezoelectric in the transducer stimulate that reaction. There is a presence of a dense precipitate of Cu_xS_y at the surface of the transducer after the experiments. It seems that copper reacts with sulphur to form a Cu_2S precipitate at

Table 1. Overview of solvents parameters for ultrasonic spray pyrolysis at 25 °C.

Solvent	σ [N/m]	ρ [kg/m^3]	f [Hz]	D [m]
Water	71.97 x 10^{-3}	1x 10^3	2.35 x 10^6	2.34 x 10^{-6}
			2.6 x 10^6	2.19 x 10^{-6}
Methanol	22.5 x 10^{-3}	0.791 x 10^3	2.35 x 10^6	1.72 x 10^{-6}
			2.6 x 10^6	1.6 x 10^{-6}

Figure 3. XRD spectra of ITO substrate and films deposited from aqueous precursors solution with different precursors' ratio of copper, indium and sulphur.

the transducer surface according to the reaction.

This indicates that there is less copper and sulfur in the droplets which form the mist created by the aqueous precursors solution.

The characterization of the CIS1 (thin films obtained after 3 minutes of wetting the substrate surface) and CIS2 (thin films obtained after 7 minutes of wetting the substrate surface) samples, obtained from the aqueous precursors solutions, shows similar results. The characterization of the CIS1 and CIS2 samples, obtained from the alcoholic precursors solutions, shows some differences. Therefore CIS1 and CIS2 will be related only to samples prepared from alcoholic precursor solution.

Fig. 3 shows the XRD diffraction patterns of the grown films from aqueous precursors solution. The deposit of thin film clusters begins when the ratio of precursors equals Cu:In:S = 1.2:1:3.6. As the copper and sulfur amount are increased simultaneously to maintain a ratio S/Cu = 3, the XRD pattern peaks became more significant. For a ratio Cu:In:S = 1.4:1:4.3, there was no film growth as the transducer's vibrations were disturbed by the amount of precipitate at its surface. Following this, the ratio S/In = 3.9 was maintained while the amount of copper was increased. The highest peak intensity is reached with a Cu:In:S ratio of 1.4:1:3.9. Then, as the amount of copper increases in the solution, its peak intensity decreases. According to XRD characterization, it seems that thin films are obtained with the following conditions: Cu/In ≥ 1.2; S/Cu ≤ 3 and S/In ≥ 3. The growth of a layer begins when the concentration ratio of Cu:In: equals to 1.2:1:3.6. The X-ray diffraction patterns of fig. 3 indicates the presence of a crystalline layer having diffraction peaks at 2θ = 27.29° and 32.97°. For a concentration ratio S/In = 1:3.9 and Cu/In equals 1.3 and 1.4 there is the presence of two peaks, at 2θ = 17.2° and at 2θ = 23.5°. These peaks are sharp for Cu/In = 1.4 and do not appear when Cu/In = 1.5. Comparing the positions of these peaks with the XRD database suggests that this thin layer is either indium sulfide (In_2S_3) - referring to JCPDS No. 25-0390 [19, 20] and more specifically the β-In_2S_3
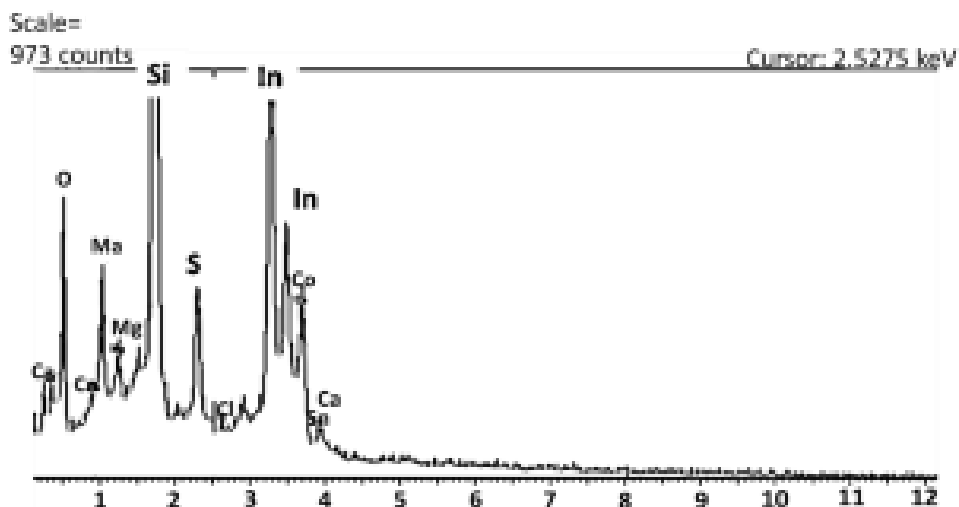
Figure 4. EDAX spectra of obtained samples from an aqueous precursors solution
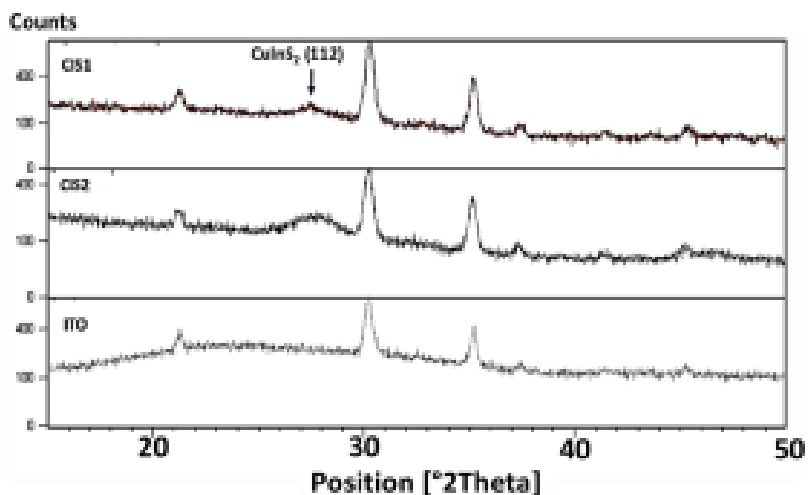
Figure 5. XRD spectra of obtained samples from alcoholic precursors solution. CIS1 stands for CuInS$_2$ prepared with 3 minutes of wetting the substrate surface, and CIS2 stands for CuInS$_2$ prepared with 7 minutes of wetting the substrate surface.

(JCPDS no. 65-0459 [21, 22]) or a ternary compound I-III-VI$_2$ consisting of copper-indium-sulfur (CIS). The various CIS that could match are CuInS$_2$, CuIn$_5$S$_8$ and CuIn$_{11}$S$_{17}$. However only the CuInS$_2$ has a diffraction peak around 2θ = 17.5 ° (JCPDS no. 27-0159 [23, 24]). The peaks located at 2θ = (21.2°, 30.5°, 35.5°) referred to ITO. Fig.4 shows the Energy-dispersive X-ray spectroscopy (EDAX) spectra of the deposited sample. Indium and sulphur are detected in the samples obtained from an aqueous precursors solution. There was no copper detected in the thin films whatever the amount of copper in the precursors solution. It looks like all the copper reacted with sulphur to form the white precipitate that stayed at the surface of the transducer. Thus the XRD and EDAX spectra indicate that the obtained thin films are In$_2$S$_3$.

The particle sizes were determined by the Scherrer equation (D=Kλ/(β cos θ) [25], where D is the grain size, K is a dimension-

less shape factor, λ is the X-ray wavelength, θ is the Bragg angle and β is the line broadening at half the maximum intensity (FWHM), in radians. For the samples obtained from a precursors ratio Cu:In:s = 1.4:1:3.9, the average grain size is of order of 220 Å and the thin film thickness is of order of 812 nm.

Fig. 5 shows the XRD spectra of samples obtained from alcoholic precursors solution. According to these results, the obtained films from alcoholic precursors solution (CIS1 and CIS2) are CuInS$_2$. The peaks obtained showed that the preferred orientation is (112). The average grain size was found to be of order of 110 Å. The average thickness, determined with the Keyence 3D Laser Scanning Microscope, was 600 ± 20 nm.

The nature of the obtained film, determined by XRD, is confirmed to be a CuInS$_2$ by the Energy-dispersive X-ray spectroscopy (EDAX). Figs.6a and 6.b show the EDAX spectra of the sample

a)

b)
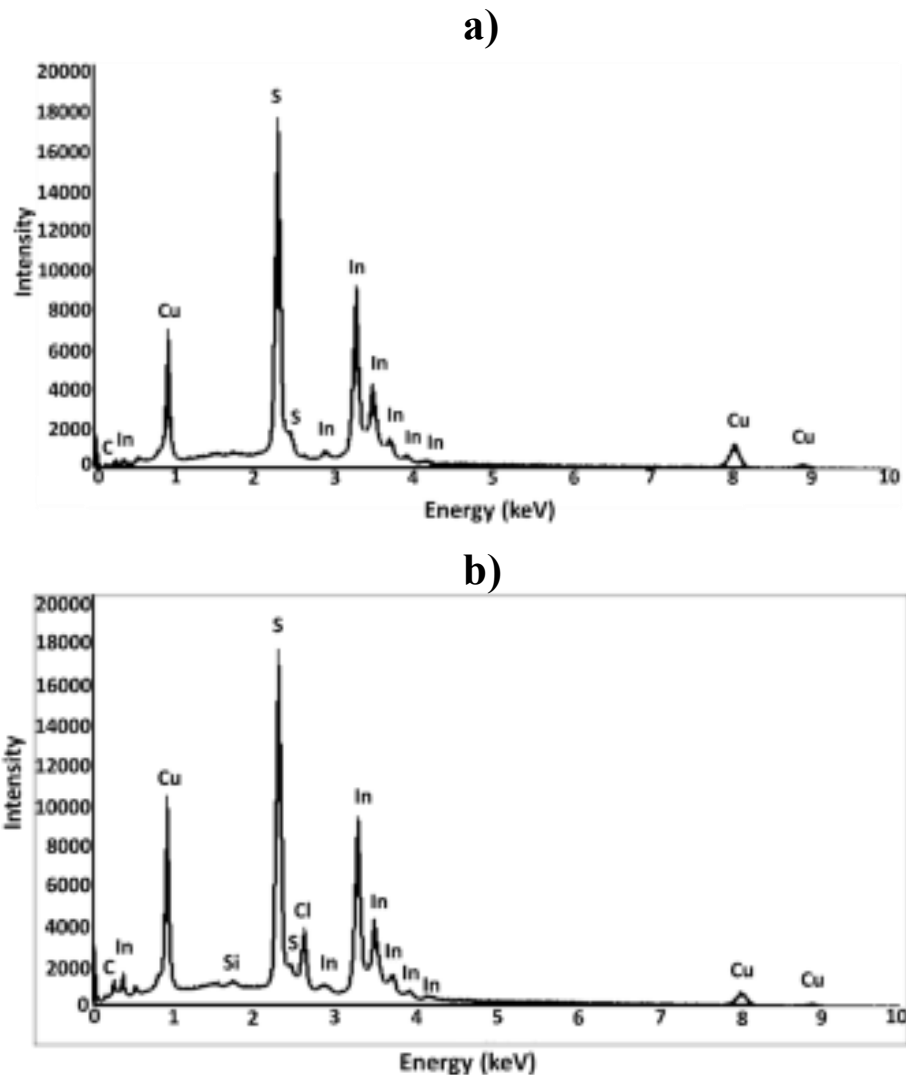
Figure 6. EDX spectrum of obtained samples with methanol as solvent; a) CIS1 for $CuInS_2$ prepared with 3 minutes of wetting the substrate surface, and: b) CIS2 for $CuInS_2$ with 7 minutes of wetting the substrate surface.

which indicate the presence of indium, sulfur and copper in the films prepared from alcoholic precursor solution. However, the chlorine is detected on CIS2 samples, as seen in figure 6.b. It might be assumed that wetting the substrate surface during 7 minutes could promote the presence of this specie, which comes from the precursor, at the surface of the substrate.

The chemical composition of the sample obtained from the EDAX semiquantitative analysis is shown in table 2. It shows that the duration of the wetting process allows the bonding of more copper and sulphur elements at the surface.

In the four points probe technique, the intensity of the current is linked to the variation in potential by the equation

$$\frac{V}{1} = K \frac{\rho}{d} \qquad (2)$$

where V (V) is the potential, I (A) – the current intensity, ρ (Ω.cm) - the electrical resistivity and d (cm) is the thickness. K is a dimen-

sionless coefficient characteristic of the sample geometry and, for an endless layer (infinite) [26, 27]:

$$K = \ln(2)/\pi \qquad (3)$$

The average samples resistivity is approximately equal to 1.3 x 10^4 Ω.cm which is similar to values reported for $CuInS_2$ films prepared by spray [28, 29] and reactive sputtering [30]. This high value of resistivity could be explained by the grain size of these films

Table.2 Semiquantitative comparison of the elements copper, indium and sulfur present in obtained thin layers.

Cu:In:S precursor ratio	Sample	S	In	Cu	Cu : In : S
1:1:4	CIS1	53	30.3	16.7	1 : 1.8 : 3.2
	CIS2	48.24	28.64	23.12	1 : 1.2 : 2
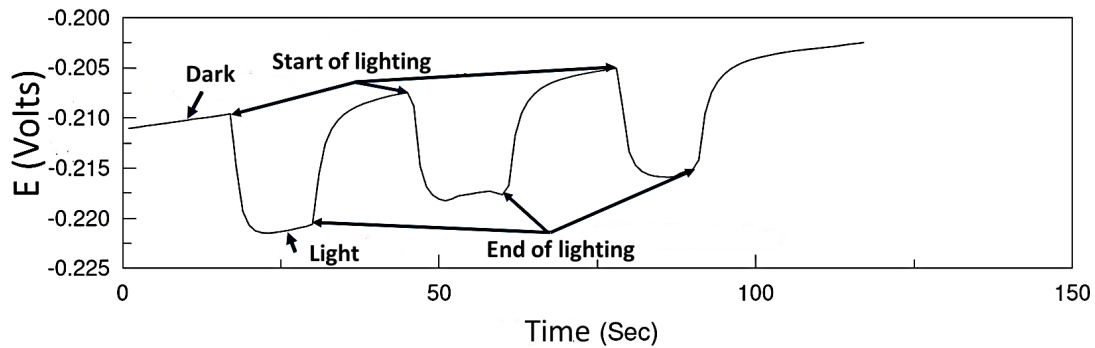
Figure 7. Effect of the chopped illumination with 100mW/cm^2 Xenon lamp on the response of the interface of 1M NaOH/CuInS$_2$ of the voltage vs time.
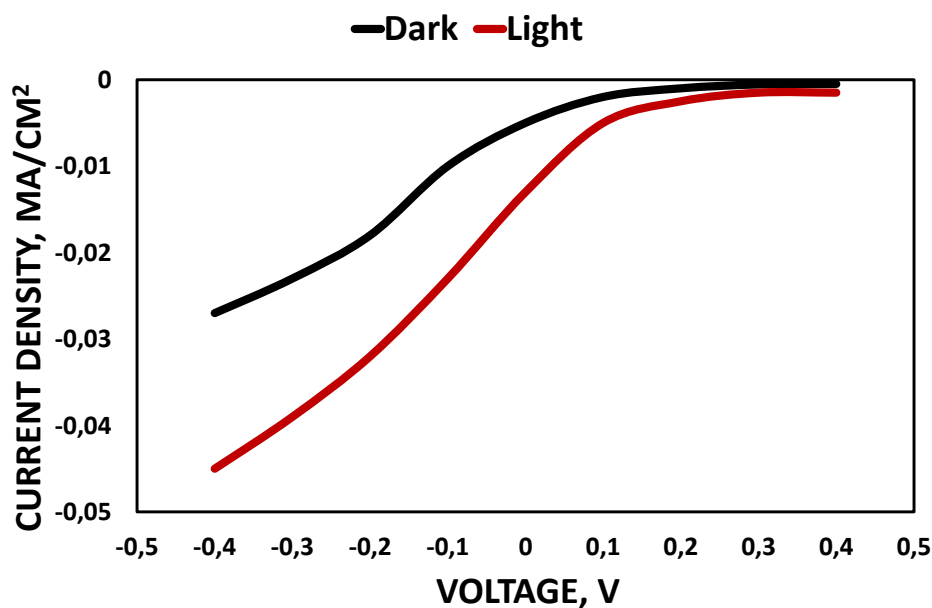
Figure 8. Current-voltage characterization under dark and illumination of the 1 M NAOH/p-CuInS$_2$ based photoelectrochemical cell (PEC)

and/or, by some compensation effects resulting from the reduction of acceptor states (copper vacancies) by the occupation of indium atoms (creation of donor states) [29, 31].

To determine the conductivity type of obtained films, using a potentiometer, we studied their electrical behaviour both in darkness and under illumination. The conductivity type of the films was determined by photocurrent characterization. The Princeton Applied Research potentiostat was used for photocurrent measurements. The characterization was carried out in a custom built photoelectrochemical cell with a Platinum mesh, Ag/AgCl reference electrode, and the CuInS$_2$ sample as the counter, reference, and working electrode, respectively. The electrolyte was an aqueous solution of 1 M NaOH. The illumination of the semiconductor electrolyte interface was realised using a xenon lamp through the electrolyte with an incident light of 100 mW/cm^2. The lamp switch was manually controlled to chop the light at certain time intervals. The electrical response of the samples is shown in figure 7. From

there, it is possible to determine that for each chopped light, the difference (V$_{ph}$) of the value of the potential between illumination and the darkness is approximately -12.5 mV. The negative sign indicates that the charge carriers move from the cathode to the anode. They therefore have a positive sign. This implies that the charge carriers are holes from which one can conclude that the resulting films are p-type semiconductors.

For a p-type semiconductor electrode, the photopotential obtained under illumination, is related to a shift in the Fermi level of the nanoporous film substrate [32]. This photopotential is the absolute value of the difference between the potential in those under illumination and those under darkness. In this case, the free holes contribute in the relative value of this response. In an ideal case, the relation between the photopotential and the concentrations of charge carriers can be expressed as [32-34]:

$$V_{ph} = E_{oc}^{dark} - E_{oc} = \frac{kT}{q} \ln\left(1 + \frac{P_{v,ph}}{P_{v,dark}}\right) \qquad (4)$$
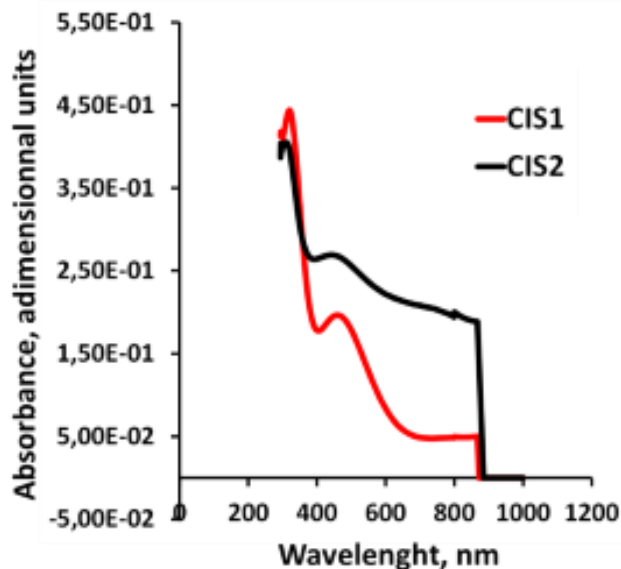
Figure 9. Absorbance spectra of CuInS₂ samples: a) CIS1 for CuInS$_2$ prepared with 3 minutes of wetting the substrate surface, and: b) CIS2 for CuInS$_2$ with 7 minutes of wetting the substrate surface.

where $p_{v,ph}$ and $p_{v,dark}$ are the valence band hole concentrations upon illumination and in the dark. The value of $p_{v,ph}$ will be given by

$$p_{v,ph} = p_{v,dark}\left(e^{\frac{qV_{ph}}{kT}} - 1\right) = 0.65 p_{v,dark} \qquad (5)$$

Thus under illumination, there was an increase of the concentration of charge carriers, i.e. holes, of the order of 65 %. However the eq. (5) ignores recombination phenomena, hence the need to develop an equation (in development) which involves a constant reaction that takes into account the recombination processes.

The figure 8 shows a significant increase of the current under illumination compared to the current under darkness. This confirms the p-type nature of the obtained CuInS$_2$ films.

The absorption spectrum e.g. the variation of the absorbance with the monochromatic wavelength is illustrated on figure 9 for both CIS1 (CuInS$_2$ prepared with 3 minutes of wetting the substrate surface) and CIS2 (CuInS$_2$ with 7 minutes of wetting the substrate surface). The absorbance of the CIS1 sample is lower than that of the CIS2 sample. Referring to the Beer-Lambert law [35-37], the absorbance is related to the thickness by the relation:

$$A = \varepsilon t C \qquad (6)$$

where A is the absorbance, ε ($l \cdot mol^{-1} \cdot cm^{-1}$) - the molar extinction coefficient, t the thickness (cm) and C (mol·l^{-1}) the molarity.

Then, the difference in the absorbance spectra might be related to the sample thickness i.e CIS1 is thinner than CIS2. The two spectra exhibit the same cut-off at the wavelenght (λ) of 890 nm.

The Tauc plot method was used to determine the bandgap value for both samples using Tauc relation for direct bandgap transition [38-41]:

$$(\alpha h\upsilon)^2 = K(h\upsilon - E_G) \qquad (7)$$

Where α is the absorption coefficient, K – a constant and E_G (eV) is the band gap energy and $h\upsilon$ is obtained from the classical relation :

$$\lambda(nm) = \frac{1.24}{h\upsilon(eV)} \qquad (8)$$

where λ is the wavelength and $h\upsilon$ the incident photon energy.

The absorption coefficient might be related to the absorbance by one of the following relations

$$\alpha = 2.303 \frac{A}{t} \quad [42,43] \qquad (9)$$

or

$$\alpha = \frac{1}{t}\ln\left(\frac{A}{T}\right) = \frac{1}{t}(2.303A + \ln A) \quad [44,45] \qquad (10)$$

where A is the absorbance, t – the thickness and T – the transmittance of the film [36, 37]:

$$T = 10^{-A} \qquad (11)$$

The plots of $(\alpha h\upsilon)^2$ versus $h\upsilon$ are shown in Fig. 10 (a and b). In Fig. 10.a, the absorption coefficient is related to the absorbance by the relation (9), therefore $(\alpha h\upsilon)^2$ curve can be replaced by $(Ah\upsilon)^2$ curve. In figure 10.b, the absorption coefficient is related to the absorbance by the relation (10). From these figures, in our case, only the relation (9) is suitable for the application of Tauc plot method. Thus, from the Fig 10.a, the obtained material is a semiconductor with a bandgap value of 1.40 eV.

The density of holes in the valence band is determined by the product of the density of states, N_v, and their occupation probability [34], so that

$$p = N_v exp\left(\frac{E_V - E_F}{k_B T}\right) \qquad (12)$$

Under darkness, the Fermi level is equal to the redox Fermi level, $E_{F,redox}$ [34] and the hole density is determined by

$$p_{v,dark} = N_v exp\left(\frac{E_V - E_{F,redox}}{k_B T}\right) \qquad (13)$$

Using the recombination-generation model, the recombination rate has its maximum where n = p, or approximately where [1, 46]

$$E_F = (E_v + E_c)/2 \qquad (14)$$

Then we obtain the following equation [47]

$$p_{v,dark} = N_v exp\left(\frac{E_V - E_{F,redox}}{k_B T}\right) = N_v exp\left(\frac{2E_V - E_V - E_C}{2k_B T}\right) =$$

$$= N_v exp\left(\frac{E_V - E_C}{2k_B T}\right) = N_v exp\left(-\frac{E_G}{2k_B T}\right) \qquad (15)$$

The lifetime of minority carrier (the electrons in p-CuInS$_2$) is

a)

b)
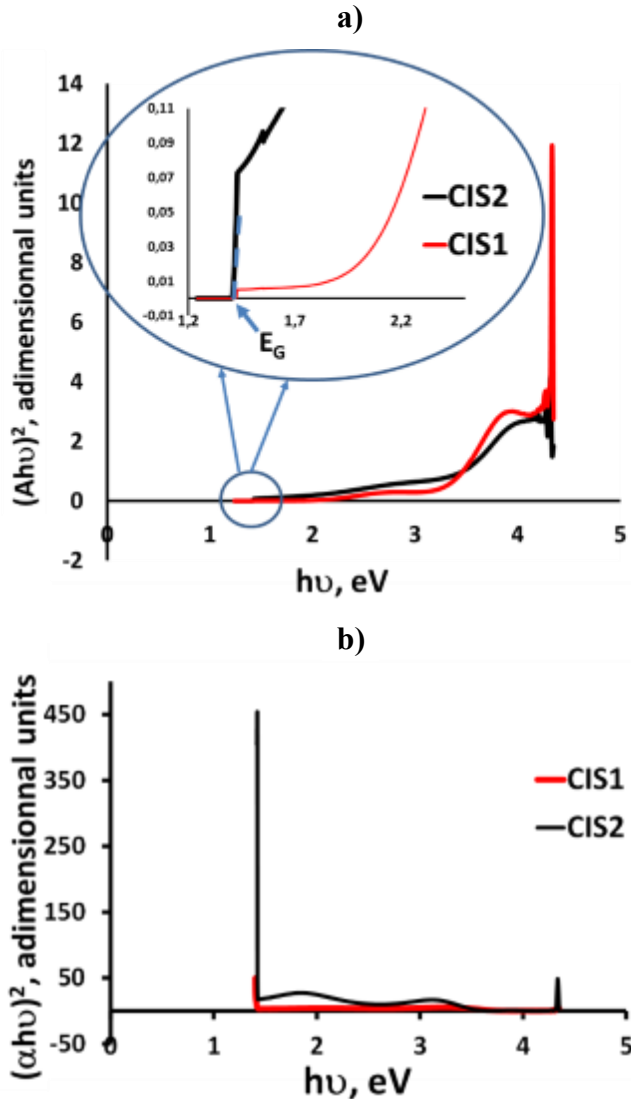
Figure 10. Tauc plot of CuInS₂ samples. a) curve obtained using a = 2.303A/t, and b) curve obtained using a = 1/t (2.303A + ln A). CIS1 indicates CuInS₂ samples prepared with 3 minutes of wetting the substrate surface, and CIS2 indicates CuInS₂ samples prepared with 7 minutes of wetting the substrate surface.

therefore equal to that of the excess of charge carriers (photogenerated carriers) , i.e [48]

$$R = \frac{n_{e} - n_{e,dark}}{\tau_{n}} = G = \alpha \frac{P_{opt}}{E_{ph} S} \qquad (16)$$

Where R is the recombination rate, n_e – electron concentration under illumination, $n_{e,dark}$ – the electron concentration in the dark, τ_n – the minority carrier lifetime, G the generation rate, P_{opt} – the illumination power, S the surface sample area and E_{ph} – the photo energy obtained at the absorption coefficient α.

$$n_e - n_{e,dark} = p_v - p_{v,dark} = 65\ \%\ p_{v,dark} \qquad (17)$$

where p_v is the holes concentration upon illumination. However the relation (17) ignores recombination phenomena, hence the need to develop an equation (in development) which involves a constant reaction that takes into account the recombination processes. From eq. (16) and eq. (17) the lifetime of minority carrier t_n is then given by the relation

$$\tau_n = \frac{0.65\, p_{v,dark}\, E_{ph}\, St}{2.303A\, P_{opt}} \qquad (18)$$

At room temperature, the density of states is given by the equation [42]:

$$N_v = 2\frac{(2\pi m_p^* k_B T)}{h^2}$$

$$\qquad (19)$$

$$= 2\frac{(2\pi 1.3 \times 9.11 \times 10^{-31} \times 1.38 \times 10^{-23} \times 300)}{(6.626 \times 10^{-34})^2} = 3.72 \times 10^{19}\ cm^{-3}$$

With $m_p^* = 1.3\ m_0$ [49] where $m_0 = 9.11 \times 10^{-31}$ kg is the free electron rest mass [48].

Then, from eq. (15) we obtained $p_{v,dark} = 6.5 \times 10^7\ cm^{-3}$.

According to Fig 9, regarding CIS2, for $A = 0.2$, $l = 800$ nm => $E_{ph} = 1.55$ eV.

Then from eq. (18) we obtained $\tau_n = 1.36 \times 10^{-14}$ s.

This value is lower than those obtained in the literature [48, 50, 51] but might be explained by the fact that the recombination processes were not taken in account and it was assumed that the Fermi level was at the position where the concentration of holes (p) is equal to the concentration of electrons (n), therefore the recombination rate is at its maximum.

4. CONCLUSION

The EDS and XRD spectra indicate that In₂S₃ clusters were grown from aqueous precursor solution and that CuInS₂ thin films were grown from alcoholic (methanol) precursor solution. The lack of copper in the samples prepared from the aqueous solution may be linked to the formation of Cu$_x$S$_y$ precipitate in the piezoelectric system at the vibrating surface of the transducer. Accordingly the concentration of the copper in the deposition mist at the surface is significantly decreased and the copper in the deposit at the surface is so low it cannot be detectable. Secondly, the difference of the type and composition of the deposits, cluster and thin film, are related to the solvent type and composition at the temperature of the deposition. Methanol inhibits the reaction between the precursors and evaporates very fast so that the reaction between the precursors takes place at the substrate surface and allow the growth of a film. Water evaporates more slowly than methanol so that the reaction between precursors occurs in the solvent, while in the droplet state and then a cluster is deposited. So, when used with alcoholic solvent, Transducer-based ultrasonic spray pyrolysis (TUSP) is a technique that allows the deposition of p-CuInS₂ very thin and transparent films with a band-gap value of 1.40 eV and a smooth homogenous surface. The minority carrier lifetime was also estimated. Thus TUSP might be suitable for the deposition of CuInS₂ on a nanoporous semiconducting materials without clog-

ging or blasting the pores. Indeed, TUSP can be used for the growth of CuInS$_2$ thin film as extremely thin absorber for application in 3D solar cells technology.

REFERENCES

[1] A. Neisser, "Gallium as an isovalent substitution in CuInS$_2$ absorber layers for photovoltaic applications", Ph. D. dissertation, Freie Universität Berlin, Berlin, Germany, 2001.

[2] A. Goossens, J. Hofhuis, Nanotechnology, 19, 424018 (2008).

[3] J. Klaer, J. Bruns, R. Henninger, K. Siemer, R. Klenk, K. Ellmer, D. Bräunig, Semiconductor Science and Technology, 13, 1456 (1998).

[4] L. Reijnen, B. Feddes, A. M. Vredenberg, J. Schoonman, A. Goossens, The Journal of Physical Chemistry B, 108, 9133 (2004).

[5] M. Nanu, J. Schoonman, A. Goossens, Advanced Materials, 16, 453 (2004).

[6] I. Kaiser, K. Ernst, C. H. Fischer, R. Könenkamp, C. Rost, I. Sieber, M. C. Lux-Steiner, Solar Energy Materials and Solar Cells, 67, 89 (2001).

[7] S. F. Buecheler, "Investigation of compound semiconductors as buffer-layer in thin film solar cells", Ph. D. dissertation, ETH Zürich, Zürich, Switzerland, 2010, p. 153.

[8] K. Ernits, M. Kaelin, D. Brémaud, T. Meyer, U. Müller, A. N. Tiwari, in "Proceedings of the 21st European Photovoltaic Solar Energy Conference and Exhibition", Eds. J. Poortmans, H. Ossenbrink, E. Dunlop and P. Helm, Dresden, Germany, 2006, p. 4.

[9] M. Kaelin, D. Rudmann, A. N. Tiwari, Solar Energy, 77, 749 (2004).

[10] J. H. Bang, Y. T. Didenko, R. J. Helmich, K. S. Suslick, Material Matters 7, 15 (2012).

[11] D. Perednis, L. J. Gauckler, Journal of Electroceramics, 14, 103 (2005).

[12] E. Aydin, N. D. Sankir, Journal of Optoelectronics and Advanced Materials, 15, 14 (2013).

[13] S. Buecheler, D. Corica, D. Guettler, A. Chirila, R. Verma, U. Müller, T. P. Niesen, J. Palm, A.N. Tiwari, Thin Solid Films, 517, 2312 (2009).

[14] T. Saeed, "New routes to II-VI materials", Ph. D. dissertation, University of London, London, England, 1995.

[15] M. Dudita, L. Isac, A. Duta, Bulletin of Materials Science, 35, 997 (2012).

[16] C. Jiang, W. L. Koh, M. Y. Leung, W. Hong, Y. Li, J. Zhang, Journal of Solid State Chemistry, 198, 197 (2013).

[17] CRC handbook of chemistry and physics, Ed. W. M. Haynes CRC PRESS, Boca Raton, USA, 2015, p. 6-186.

[18] G. Vazquez, E. Alvarez, J. M. Navaza, Journal of Chemical & Engineering Data, 40, 611 (1995).

[19] N. Allsop, C.-H. Fischer, S. Gledhill, M.C. Lux-Steiner, Patent No: US 8,143,145 B2, Berlin, Germany, 2012.

[20] JCPDS, (Joint committee on powder diffraction standards), 25-0390.

[21] M. Abd-Lefdil, C. Messaoudi, H. Bihri, S. Abd-Lefdil, D. Sayah, M. J. Condensed Matter, 1, 71 (1998).

[22] JCPDS, (Joint committee on powder diffraction standards), 65-0459.

[23] M. Abaab, M. Kanzari, B. Rezig, M. Brunel, Solar Energy Materials and Solar Cells, 59, 299 (1999).

[24] JCPDS, (Joint committee on powder diffraction standards), 27-0159.

[25] A. L. Patterson, Physical Review, 56, 978 (1939).

[26] F. Smits, Bell System Technical Journal, 37, 711 (1958).

[27] L.B. Valdes, in "Proceedings of the IRE", 42, 420 (1954).

[28] M. Krunks, A. Mere, A. Katerski, V. Mikli, J. Krustok, Thin Solid Films, 511, 434 (2006).

[29] M. Ortega-López, A. Morales-Acevedo, Thin Solid Films, 330, 96 (1998).

[30] Y. B. He, T. Krämer, A. Polity, R. Gregor, W. Kriegseis, I. Österreicher, D. Hasselkamp, B. K. Meyer, Thin Solid Films, 431, 231 (2003).

[31] H. Y. Ueng, H. L. Hwang, Journal of Physics and Chemistry of Solids, 50, 1297 (1989).

[32] D. Monllor-Satoca, R. Gomez, The Journal of Physical Chemistry C, 112, 139 (2008).

[33] R. Gómez, P. Salvador, Solar Energy Materials and Solar Cells, 88, 377 (2005).

[34] L. M. Peter, solar cells, Physical Chemistry Chemical Physics, 9, 2630 (2007).

[35] F. Guedira, in "Cours de Spectroscopie", Faculté des Sciences de Rabat, Université Mohammed V, Rabat, Maroc, 2013, p. 18.

[36] P. Bouguer, "Essai d'optique sur la gradation de la lumière", CLAUDE JOMBERT, Paris, France, 1729.

[37] Klett, E. Witwe, Detleffsen, C. Peter, I. H. Lambert, "Photometria sive de mensura et gradibus luminis, colorum et umbrae", SUMPTIBUS VIDUAE EBERHARDI KLETT, Augsburg, Germany, 1760.

[38] K. Füchsel, U. Schulz, N. Kaiser, A. Tünnermann, Appl. Opt., 47, C297 (2008).

[39] O. Stenzel, "The physics of thin film optical spectra: an introduction", SPRINGER, Berlin, Germany, 2005.

[40] J. Tauc, in "Optical properties of solids", Ed., F. Abeles, NORTH-HOLLAND, Amsterdam, Holland, 1972.

[41] J. Tauc, R. Grigorovici, A. Vancu, physica status solidi (b), 15, 627 (1966).

[42] M. N. Al-Jabery, Q. A. Abbas, H. S. Al-Jumaili, Iraqi Journal of Physics, 10, 70 (2012).

[43] J. -Y. Park, J. -P. Park, C. -H. Hwang, J. -E. Kim, M. -H. Choi, K. -M. Ok, H. -Y. Kwak, I. -W. Shim, Bulletin of the Korean Chemical Society, 30, 2713 (2009).

[44] S. Thanikaikarasan, T. Mahalingam, S. Lee, H. Lim, S. Velumani, J. -K. Rhee, Materials Science and Engineering: B, 174, 231 (2010).

[45] S. Thanikaikarasan, T. Mahalingam, Journal of Alloys and Compounds, 511, 115 (2012).

[46] R. Klenk, Thin Solid Films, 387, 135 (2001).

Characterization of CuInS₂ Thin Films Grown by Transducer-based Ultrasonic Spray Pyrolysis for PV Solar Cells Applications
/ J. New Mat. Electrochem. Systems

179

[47] J. -P. Colinge, C. A. Colinge, Physics of Semiconductor Devices, Springer, 2002.

[48] B. Van Zeghbroeck, Principles of electronic devices, University of Colorado, (2011).

[49] Landolt-Börnstein, in "Ternary Compounds, Organic Semiconductors", Eds., O. Madelung, U. Rössler, M. Schulz, SPRINGER BERLIN HEIDELBERG, Berlin, Germany, 2000, p. 1.

[50] A. Opanowicz, B. Kóscielniak-Mucha, physica status solidi (a), 105, K135 (1988).

[51] A. R. Warrier, K. Deepa, T. Sebastian, C. S. Kartha, K. P. Vijayakumar, Thin Solid Films, 518, 1767 (2010).